

**ROBUST MAGNITUDE AND PATH CORRECTIONS FOR REGIONAL SEISMIC PHASES IN EURASIA  
BY CONSTRAINED INVERSION AND ENHANCED KRIGING TECHNIQUES**

Mark D. Fisk<sup>1</sup> and Steven R. Taylor<sup>2</sup>

ATK Mission Research<sup>1</sup> and Rocky Mountain Geophysics, LLC<sup>2</sup>

Sponsored by National Nuclear Security Administration  
Office of Nonproliferation Research and Development  
Office of Defense Nuclear Nonproliferation

Contract No. DE-AC52-06NA27321

**ABSTRACT**

This project is to develop and test two methods to improve magnitude and path corrections for regional seismic phase amplitudes. Objectives of the first method, a constrained inversion approach, are to improve estimates of geometrical spreading and  $Q$  for Pn, Pg, Sn, Lg in Eurasia, by eliminating trade-offs with source corner-frequency estimates, and to improve source parametrizations, in terms of grids of stress drop and corner frequency scaling. Using waveform cross-correlations from Dr. Schaff of Lamont-Doherty Earth Observatory for 4,236 events prior to 2000 in Eurasia, (1) data were obtained for event pairs or clusters in a data set from Los Alamos National Laboratory (LANL); (2) additional seismograms from IRIS were incorporated; (3) regional phase picks were added; (4) network-averaged relative spectra (for large-over-small event pairs) were processed for Pn, Pg, Sn and/or Lg; and (5) relative spectra of a Brune model were fit to the empirical relative spectra. Cases were considered with the apparent stress-drop scaling parameter,  $\psi$  (as defined by Walter and Taylor, 2002), as a free parameter or fixed at 0.0 or 0.25. Preliminary kriged grids of stress drop have been computed for Eurasia, based on relative spectra for individual phases and combining the results for the various phases. The results thus far seem to show that the scaling of corner frequency with seismic moment for earthquakes is very consistent among the various regional phases. An interesting observation is that the estimated P- and S-wave corner frequencies for a given event are very similar for a majority of earthquake pairs throughout many diverse areas of Eurasia, comparable to findings by Walter and Taylor (2002) for western U.S. earthquakes. Important implications of this result are discussed. These analyses have been automated and are being applied to almost 3600 earthquake pairs in Eurasia from 2000 to 2007.

The objective of the second method, an extension to Bayesian kriging, is to provide robust path corrections and uncertainties for regional seismic phase amplitudes that properly treat localized calibration events which may have anomalous, correlated amplitudes. To first demonstrate the problem, a Bayesian kriging approach is applied to explosions and clusters of earthquakes with distinct focal mechanisms at the Nevada Test Site (NTS), including a cluster of Rock Valley earthquakes with anomalously high P/Lg values. The results indicate that explosions can be mis-categorized as earthquakes when using such earthquake clusters for kriging because the localized reference data is weighted too high in estimating the corrections and the posterior calibration variance becomes too small. To address this issue, a fundamental improvement to the kriging methodology, incorporating an additional correlation length to treat correlated focal mechanisms, is presented and tested on the NTS data sets and on large samples of explosions and earthquakes worldwide. Application to the worldwide data sets indicates that the power of the hypothesis test to reject earthquakes as explosions is marginally reduced, without mis-categorizing any known explosions and providing a robust treatment of clustered reference data.

## **OBJECTIVES**

We are developing and testing two methods to improve magnitude and path corrections for regional seismic phase amplitudes. Objectives of the first method, a constrained inversion approach, are to improve estimates of geometrical spreading and Q models for Pn, Pg, Sn, Lg in Eurasia, by eliminating trade-offs with source corner frequencies, and to improve source parametrizations in Eurasia, in terms of grids of stress drop and corner frequency scaling. The objective of the second method, an extension to Bayesian kriging, is to provide robust path-specific corrections and uncertainties for regional phase amplitudes, that properly treats localized calibration events that may have anomalous, correlated amplitudes. This project has three main tasks: (Task 1) Assemble multiple data sets of regional seismic recordings of earthquakes throughout broad areas of Eurasia. Apply waveform cross-correlation techniques to determine nearby pairs/clusters of events. Assemble spectral amplitude measurements of Pn, Pg, Sn, Lg for the events. (Task 2) Implement a technique to estimate corner frequencies and scaling parameters for Pn, Pg, Sn, Lg, by fitting relative spectra of a Brune model to data for pairs of nearby earthquakes of different moments. Compute grids of stress drop and earthquake corner-frequency scaling with moment for Eurasia. Use spectral amplitude data for regional phases and constrained source parametrizations to perform a robust inversion for geometrical spreading and Q model parameters. Test and evaluate resulting magnitude and distance corrections on events in Eurasia, using cross-validation methods. (Task 3) Investigate clusters of earthquakes at NTS and regions in Eurasia, and assess the potential for events with anomalous, correlated mechanisms to bias kriged amplitude correction grids beyond existing uncertainty estimates. Develop a technique to quantify the correlation of regional phase amplitudes within clusters. Extend a Bayesian kriging method to incorporate these correlation measures in the computation of amplitude correction and uncertainty grids. Test and evaluate the methods on events in Eurasia, using cross-validation techniques. We plan to deliver the techniques, parametrizations of stress drop, corner frequency scaling, geometrical spreading and Q models, and kriged amplitude correction and uncertainty grids for stations in Eurasia.

## **RESEARCH ACCOMPLISHED**

### *Constrained Inversion Technique*

Following Taylor et al. (2002), the amplitude spectrum for a given phase and station, for event  $i$ , may be expressed as

$$A_i(f) = S_i(f, f_c) G(r_i, r_0) \exp\left(-\frac{\pi f}{Q(f)v} r_i\right) P(f) \quad , \quad (1)$$

where  $f$  is the frequency,  $S_i(f, f_c)$  is the source spectrum with corner frequency  $f_c$ ,  $r_i$  is the epicentral distance,  $v$  is the group velocity,  $P(f)$  is a unitless station term,  $Q(f) = Q_0 f^\gamma$  is the frequency-dependent attenuation, and  $G(r, r_0)$  is the frequency-independent geometrical spreading, assumed to be inversely proportional to distance to a power  $\eta$ , beyond a reference distance  $r_0$ . Taylor et al. (2002) and others have used the logarithm of Equation (1) in a grid-search procedure to simultaneously estimate all of the parameters. However, significant trade-offs between Q and corner frequencies are known to exist and are difficult to constrain by standard techniques and available data (e.g., Taylor and Hartse, 1998). This can lead to improperly correcting regional amplitudes for distance and magnitude.

Instead of performing a grid search for all parameters simultaneously, we use relative spectra for event pairs with similar locations and mechanisms, but different moments, to factor out path and station effects and estimate the source parameters. We then constrain the source parameters and invert for values of  $\eta$ ,  $Q_0$ , and  $\gamma$ . That is, for a pair of nearby earthquakes with similar radiation patterns, the model relative spectra for a given phase type is given by

$$\frac{A_1(f)}{A_2(f)} = \frac{S_1(f)}{S_2(f)} = \frac{M_0^{(1)} [1 + (f/f_c^{(2)})^2]}{M_0^{(2)} [1 + (f/f_c^{(1)})^2]} \quad . \quad (2)$$

For a Brune (1970) dislocation source, the corner frequency for seismic phase type  $\xi$  is given by

$$f_c(\xi) = c_\xi v_s(\xi) \left( \frac{\sigma_b}{M_0} \right)^{1/3}, \quad (3)$$

where  $\sigma_b$  is the stress drop,  $v_s(\xi)$  is the source medium velocity for P or S waves, and  $c_\xi$  is a constant that can depend on phase type. Walter and Taylor (2002) allow for non-constant stress drop by defining the apparent stress drop for a given moment,  $M_0$ , as

$$\sigma_b = \sigma_b^{(0)} \left( \frac{M_0}{M_0^{(0)}} \right)^\psi, \quad (4)$$

where  $\sigma_b^{(0)}$  is the stress drop at reference moment  $M_0^{(0)}$ . Setting  $\log M_0^{(0)} = 15.05$  (in MKS units;  $M_W$  4.0), and using pairs of localized earthquakes, we fit  $\sigma_b^{(0)}$  and  $\psi$  to empirical relative spectra of regional phases. Figure 1 illustrates the relative spectra and model fits for an event pair in 1997. The relative spectra are quite similar for the various phases, although over different frequency ranges because of phase-dependent signal-to-noise limitations. Hence, the model fits and estimated corner frequencies are very similar. This appears to be a fairly common and important phenomenon for the earthquakes analyzed.

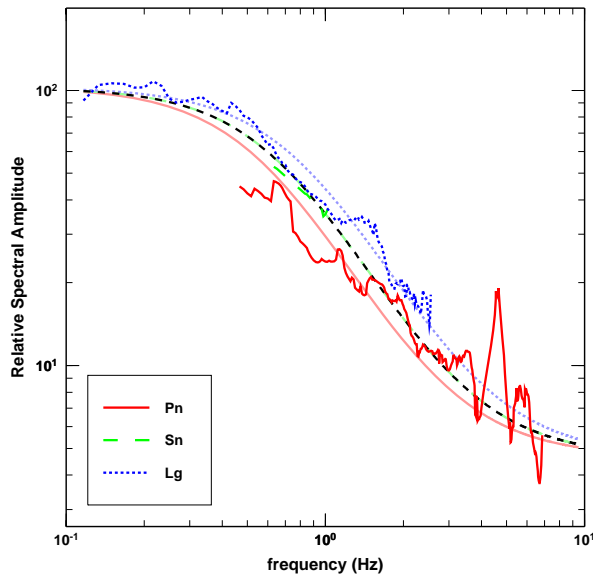


**Figure 1.** Example of relative spectra for a pair of  $M_W$  6.0 and 4.7 earthquakes in Kyrgyzstan. Model fits for each phase are represented by similar line types. The black dashed curve shows the model fit using relative spectra for all available phases.

Using waveform cross-correlations for 4,236 events in Eurasia prior to 2000 (*cf.* Schaff and Richards, 2004) to find pairs or clusters of events in the LANL database, we acquired additional seismograms from IRIS to augment the LANL data set, added and refined the regional phase picks, processed the spectra, averaged relative spectra over stations, and fit the model for each phase and using all available phases simultaneously, as in Figure 1. We allow the relative moments to be estimated directly from the relative spectra or to use moment magnitudes ( $M_W$ ) from LANL. We performed three types of fits in which the apparent stress-drop scaling parameter,  $\psi$ , is a free parameter or fixed at 0.0 or 0.25. The latter two cases correspond, respectively, to corner frequency scaling as  $M_0^{-1/3}$  (Brune, 1970) or as  $M_0^{-1/4}$  (Nuttli, 1983; Cong et al., 1996; Walter and Taylor, 2002). We computed kriged grids of stress drop for these cases.

Figure 2 shows corner frequency estimates versus log moment for Pn, Sn, and Lg for events in Eurasia, fixing  $\psi = 0$  in this case. Linear fits are shown with (dashed) and without (solid) the slopes fixed at  $-1/3$ . Given the scatter, the fits are remarkably consistent and the slope estimates are all close to  $-0.33$  for all phases. Fixing  $\psi = 0.25$ , the slope estimates are about  $-0.27$ . For  $\psi$  as a free parameter, the average value of  $\psi$  is 0.14 and the slope estimates are about  $-0.29$ . Clearly, the value of  $\psi$  affects the slope estimates of corner-frequency scaling with moment. Further work is needed to assess whether these differences are statistically significant.

Figure 3 shows that Pn and Lg corner frequencies are fairly similar for most of the earthquakes in diverse areas of Eurasia, comparable to findings by Walter and Taylor (2002) for western U.S. earthquakes. This is important for two reasons. First, it may help explain why P/S ratios discriminate effectively at higher frequencies, in most areas examined (provided path and station effects are properly treated). That is, as shown by Fisk (2006, 2007) the frequency dependence of P/S discrimination performance depends on the ratio of P- and S-wave corner frequencies squared, which is significantly larger for explosions than earthquakes at all sites examined. Thus, P/S ratios exhibit less frequency dependence for earthquakes than explosions. Second, this result may allow a more robust fitting of Brune source model parameters, using a broader range of frequencies, by

combining relative spectra of regional P and S phases for earthquakes (e.g., black dashed curve in Figure 1).

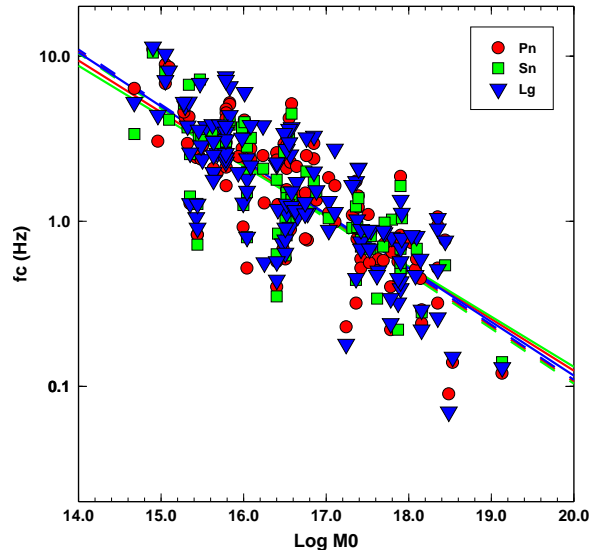


Figure 2. Corner frequency estimates versus log moment for Pn, Sn, and Lg for events in Eurasia. Linear fits are shown with (dashed) and without (solid) the slopes fixed at  $-1/3$ .

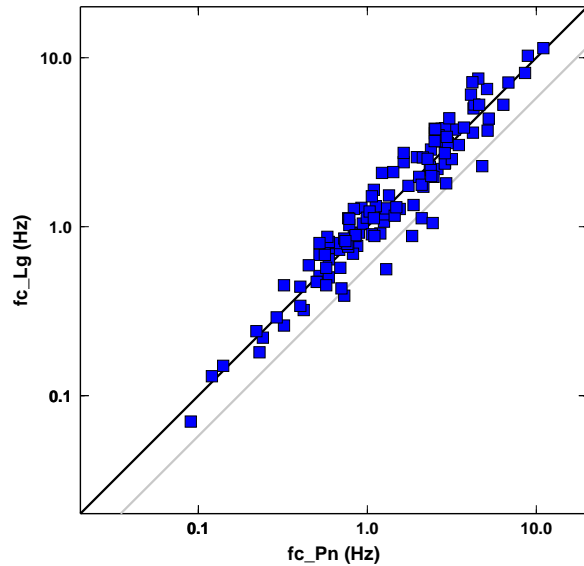


Figure 3. Estimated Lg versus Pn corner frequencies, indicating similar values for most of the earthquakes. Black and gray lines represent ratios of 1.0 and 1.73 (cf. Madariaga, 1976; Choy and Boatwright, 1995).

Figure 4 shows preliminary stress-drop grids, based on Lg and Pn data. Both grids exhibit remarkable similarity.

There is concern that some stress-drop grids might be biased, at least in certain areas, because of trade-offs with Q. Such a bias is not present in our analysis because we are using relative spectra, which factor out effects of Q. Further work is needed to incorporate much more data and interpret these stress-drop grids.

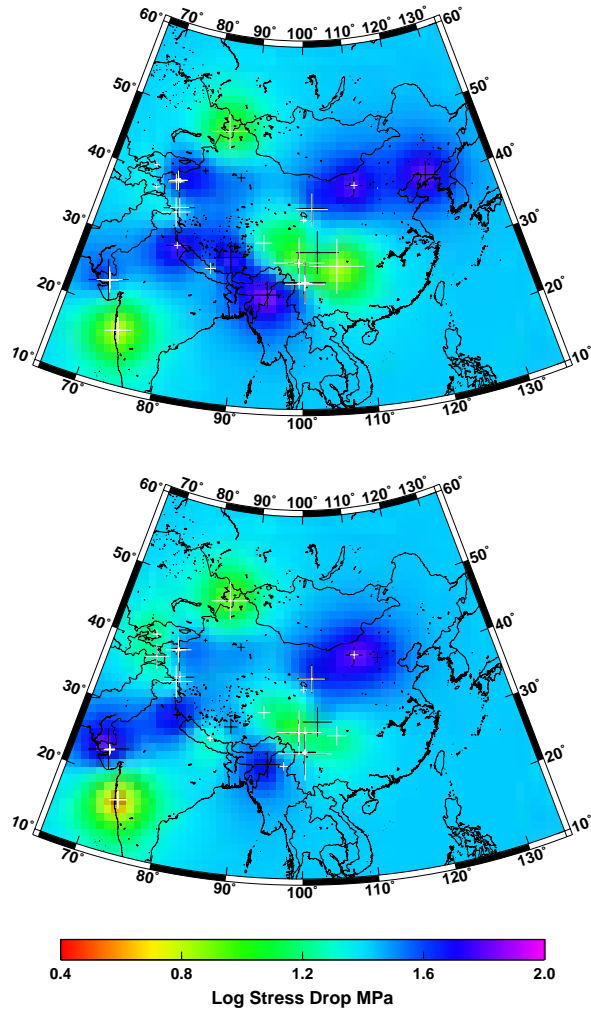


Figure 4. Kriged grids of stress drop using Lg (top) and Pn (bottom) data.

Further work is also needed to quantify the various uncertainties and the calibration and residual variances used for kriging. For some earthquake clusters, the estimated stress drops are all within about a factor of 2. For other clusters, the stress drops can vary by up to a factor of almost 60. We are examining the implications of this result on the variability and kriging of stress drop.

### *Treatment of Correlation for Clustered Reference Data in Kriging Regional Seismic Discriminants*

Despite demonstrations that kriging regional amplitudes or P/S ratios improves discrimination performance (Phillips et al., 1998; Phillips, 1999; Rodgers et al., 1998, 1999; Fisk et al., 2001; Taylor et al., 2002, Bottone et al., 2002; Fan et al., 2002), there are concerns that calibration data from events with anomalous mechanisms, depths, and/or paths could significantly bias the correction grids. The Bayesian kriging method of Bottone et al. (2002) will properly account for such situations, including computation of the uncertainties, provided the residual variance (see below) is uncorrelated. The method uses the fact that the amplitude ratios are spatially correlated, with a typical correlation length of about 600 km, corresponding largely to path variations of P/S discriminants on regional distance scales. Estimating the local corrections in this way removes about half the variance in the data. The remaining (residual) variance is treated as uncorrelated. However, for clusters of events with similar mechanisms that treatment is incorrect – there is correlation in the residual variance, although at a much shorter length scale (e.g., of faulting zones) than the variance associated with path effects. We show that ignoring this correlation can lead to serious discrimination errors, while treating it provides a robust solution at very little cost in terms of discrimination power. We first examine this issue using explosions and two aftershock sequences at NTS, including one near Little Skull Mountain (LSM) and the unusually shallow (1-3 km) Rock Valley (RV) sequence. Walter et al. (1995) showed that Pn/Lg for the RV events are considerably higher than those for the LSM events, especially at KNB. We then extend the kriging methodology by incorporating an additional correlation length to treat similar mechanisms over relatively short distance scales. We test the extended method on NTS and worldwide data sets of explosions and earthquakes and discuss implications of this study for monitoring UNEs using regional seismic P/S data.

### *Case Studies for NTS Using the Old Methodology*

We consider four cases in which only one station, either MNV or KNB, is used to monitor this area (more realistic of monitoring with a sparse global network) and either the LSM or RV events are used for kriging. For all cases, we use the distance corrections and Bayesian kriging technique, including the parameters, from Bottone et al. (2002). Figure 5 shows the grids of the corrections (left) and calibration standard deviations (right) for  $\log[\text{Pn/Lg}(6-8 \text{ Hz})]$  at MNV using 30 LSM (top) or 10 RV (bottom) earthquakes as reference events. In both cases, the corrections near NTS are fairly close to zero, the distance-corrected average for earthquakes worldwide. The calibration standard deviation near NTS for MNV, using the 30 LSM events for calibration (upper right plot), is as low as about 0.08, compared to the *a priori* value of  $\sigma_c = 0.25$  far from calibration data. Figure 6 is similar, but for station KNB using 54 LSM (top) or 11 RV (bottom) earthquakes as reference events. The most significant difference from Figure 5 is that the corrections near NTS for KNB using the 11 RV events is nearly 0.6 units higher than the corrected worldwide average for earthquakes of zero, which is 2.4 times higher than the *a priori* calibration standard deviation of 0.25.

Figure 7 shows discrimination results for the four cases, using the same procedure for all cases, except for the various correction and uncertainty grids of Figures 5 and 6. For case #1, 76 of 78 explosions (97.4%) are categorized as *explosion-like* and 26 of 40 earthquakes (65.0%) are categorized as *earthquake-like*. For case #2, 66 of 78 explosions (84.6%) are categorized as *explosion-like* and 33 of 40 earthquakes (82.5%) are categorized as *earthquake-like*. For case #3, 19 of 88 explosions (21.6%) are categorized as *explosion-like* and 39 of 65 earthquakes (60.0%) are categorized as *earthquake-like*. For these three cases, all other events are *undetermined*. These results are appropriate, given the calibration data. More importantly, no events were categorized as the incorrect event type for these three cases. However, for case #4 (lower right plot of Figure 7), although 93% of the earthquakes are categorized properly, 11 of 88 explosions (12.5%) are mis-categorized as *earthquake-like* (green stars). The problem is that the RV events have anomalously high Pn/Lg values at KNB – more than two-sigma above the worldwide average – and the posterior calibration uncertainty computed by the old algorithm is relatively small, given 11 RV reference events. The kriging calculation would be valid, if Pn/Lg data for these events were uncorrelated. However, since the RV mechanisms are correlated (Smith and Brune, 1993), the Pn/Lg data are not independent and this intrinsic correlation should be treated.

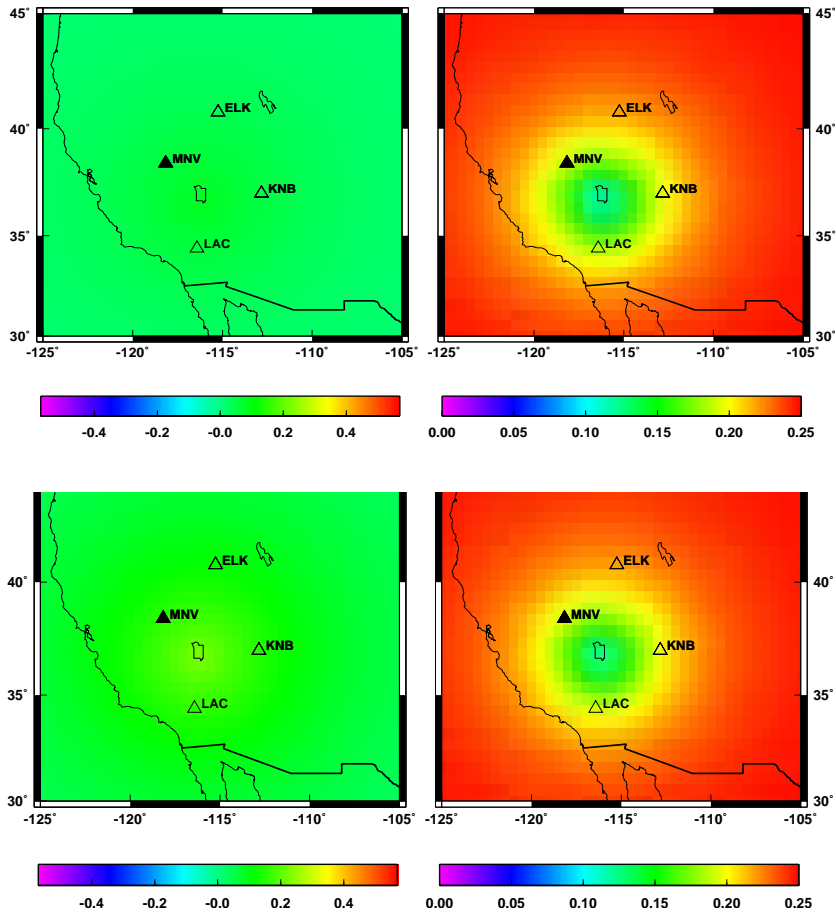


Figure 5. Kriged correction (left) and calibration standard deviation (right) grids for  $\log[P_n/L_g(6-8 \text{ Hz})]$  at station MNV, using 30 LSM (upper) and 10 RV (lower) earthquakes as reference events for the Bayesian calibration technique. The station for which the correction and uncertainty grids apply are represented by a solid triangle in each plot.

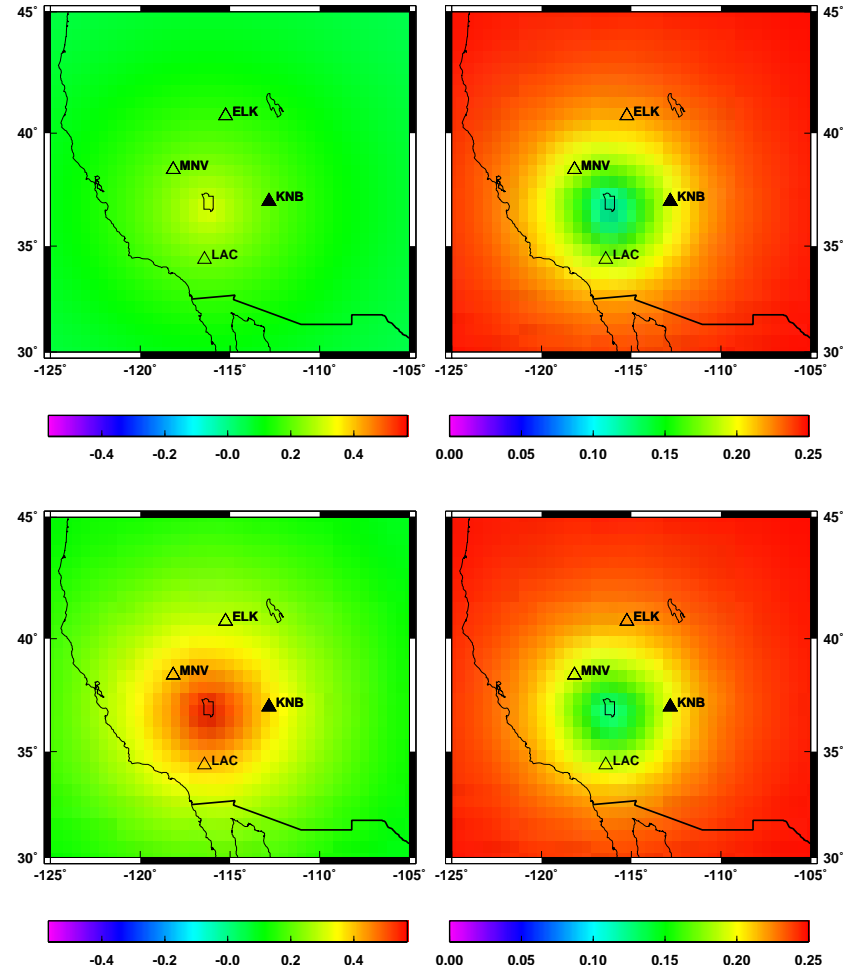
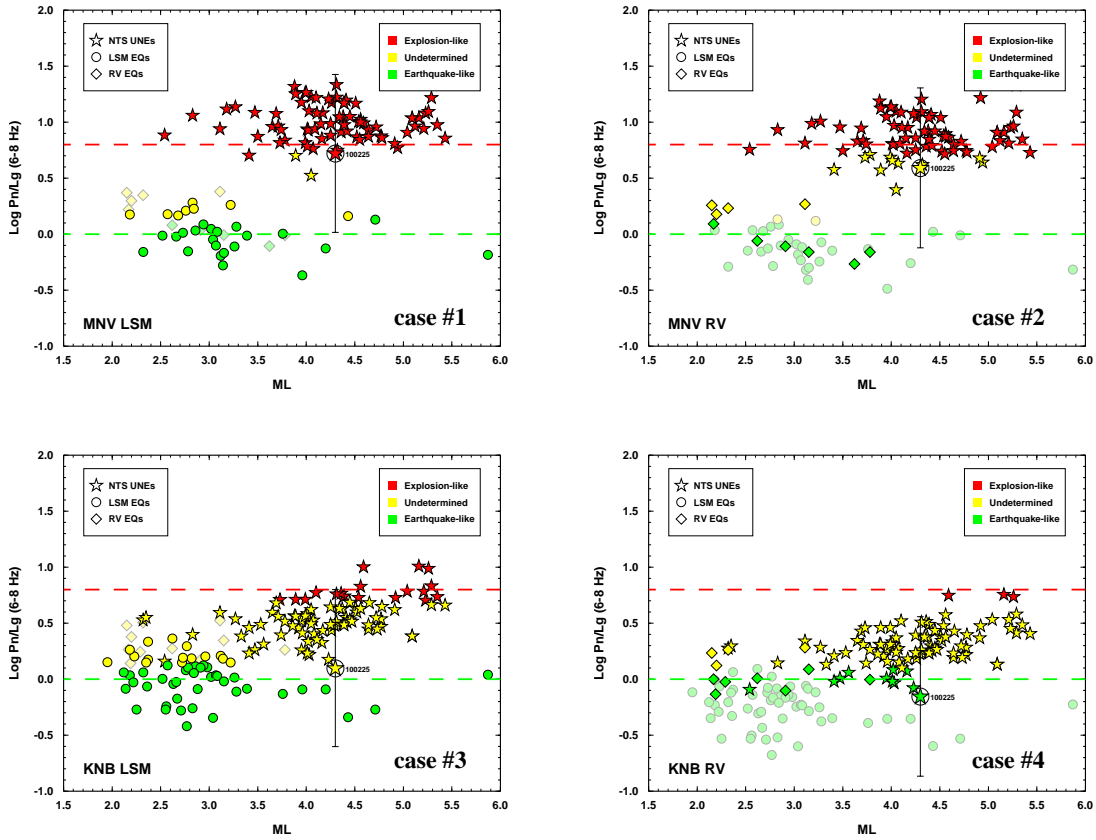


Figure 6. Similar to Figure 5, but for station KNB, using 54 LSM (upper) and 11 RV (lower) earthquakes as reference events for the Bayesian calibration technique.



**Figure 7. Discrimination results for NTS explosions and earthquakes at MNV (top) and KNB (bottom), based on the correction and uncertainty grids shown in Figures 5 and 6, using LSM (left) and RV (right) events for calibration. Faint markers correspond to events that were not used for kriging, but were tested by the discrimination criteria. Dashed lines in each plot are global means for earthquakes and explosions and the error bar represents the 99.5% confidence interval for an explosion, VILLITA.**

#### *Application of the New Methodology to NTS Events*

Bottone et al. (2002) show that the covariance,  $\Sigma$ , computed from  $N$  reference events is an  $N$ -by- $N$ -dimensional matrix with two terms,  $\Sigma^{-1} = A^{-1} + B^{-1}$ , which is used in the computation of the corrections and the posterior variance. Elements of the calibration covariance are  $B_{ij} = \sigma_c^2 \exp(-\Delta(\mathbf{s}_i, \mathbf{s}_j)/\alpha_c)$ ,  $i, j = 1, 2, \dots, N$ , where  $\Delta(\mathbf{s}_i, \mathbf{s}_j)$  is the distance between locations  $\mathbf{s}_i$  and  $\mathbf{s}_j$ . Assuming there is no correlation in the residual variance, then  $A = \sigma_r^2 I_N$ , where  $I_N$  is the identity matrix in  $N$  dimensions. If there is correlation in the residual variance, then  $A$  becomes

$$A_{ij} = \sigma_r^2 g(\Delta(\mathbf{s}_i, \mathbf{s}_j)) = \sigma_r^2 \exp(-\Delta(\mathbf{s}_i, \mathbf{s}_j)/\alpha_r), \quad (5)$$

where  $g$  is a correlation function that we have chosen to be exponential. In the limit  $\alpha_r$  goes to zero, the new formula reduces to the old one. We refer to the use of Equation (5), with nonzero  $\alpha_r$ , as the new or extended method. Physically, the original correlation length,  $\alpha_c$ , treats the effects of regional path variations on the spatial correlation of regional P/S discriminants and is estimated to be about 5 to 6 degrees for Pn/Lg and Pn/Sn in various region types (Bottone et al., 2002). The new correlation length,  $\alpha_r$ , treats correlated data for localized events, e.g., with similar focal mechanisms that typically occur on much shorter distance scales of faulting zones. Since further work is needed to estimate  $\alpha_r$ , we explore the effect of using various values in a reasonable range. It will be seen that there is little overall sensitivity to the precise value.

We now test whether the new method provides a remedy to the case of using KNB data for RV events to calibrate NTS. Even using values of  $\alpha_r$  as small as 5–6 km is sufficient so that no NTS explosions are mis-categorized as *earthquake-like*. This corresponds to inter-spatial correlation values of 0.64 to 0.96 for the RV events, with a median of 0.84. The kriged grids, computed by the new method are shown in Figure 8. The corrections and uncertainties near NTS are not affected nearly as much by the 11 RV events, relative to the worldwide prior, as before in Figure 6, since the RV data are no longer treated as independent. Now 5 of 88 NTS explosions (5.7%) are categorized as *explosion-like* and 83 are *undetermined*. Of the 65 earthquakes, 28 (43.1%) are categorized as *earthquake-like* and the remaining, including all 11 RV events, are *undetermined*. Clearly, the power of the discrimination test is quite low for this case, but note that no events are mis-categorized and this RV case is very anomalous and rare (i.e.,  $2.4\sigma_c$ ) compared to earthquakes worldwide. Below we examine the performance of the test for worldwide sets of earthquakes and explosions. Before considering that case, we also replicated the set of 11 RV earthquakes to examine whether the problem recurs if the sample of anomalous reference events becomes large. Even replicating the RV training set 20 times (i.e., 220 training samples), none of the explosions are mis-categorized and the results for the earthquakes are qualitatively the same. Thus, the improved method seems to be very robust to even large samples of anomalous reference events.

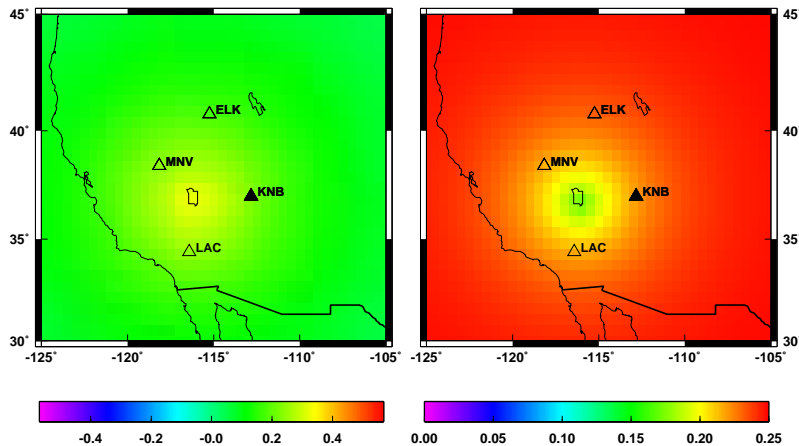


**Figure 8. Similar to Figure 6, but applying the extended kriging methodology to station KNB, using the 11 RV earthquakes as calibration events. Near NTS the correction grid does not have such high values and the uncertainty grid does not have such low values, as in the corresponding lower two plots of Figure 6.**

### Application to Worldwide Data Sets

While the previous section demonstrates a remedy to guard against mis-categorizing explosions, it remains to be seen whether the discrimination test has sufficient power to be useful in the general case, in light of the reduced power for events near NTS when the anomalous RV earthquakes are used for calibration. We now examine how the new correlation function,  $g$ , affects the performance of the event-screening procedure of Bottone et al. (2002) that was applied to worldwide sets of 4173 earthquakes and 140 explosions. For this analysis, we use the same data sets that were considered by Bottone et al. (2002). Since the specific value of the correlation length,  $\alpha_r$ , requires much more work to estimate, we apply the extended method using various values of  $\alpha_r$ . As a conservative approach, one could use a fairly large correlation length; i.e., assume that all localized sets of events might be highly correlated.

Figure 9 shows the percentage of earthquakes that are rejected as being explosions at the 0.005 significance level versus various values of the correlation length,  $\alpha_r$ , ranging from 0 to 4 degrees. The baseline case of  $\alpha_r = 0$  corresponds to the original analysis performed by Bottone et al. (2002). As expected, the power typically decreases with increasing  $\alpha_r$  because the posterior variance generally increases. However, for  $\alpha_r = 0.5$  the power of the test increases slightly as compared to the baseline case. This can occur because the posterior means at some locations also change somewhat. For a correlation length of 1.0 degree, the power decreases by only about 2%. This is quite remarkable because it suggests that a rather conservative value of  $\alpha_r$  may be used to protect against such cases as at NTS, without much degradation to the overall power of the discrimination test for broad-area monitoring.

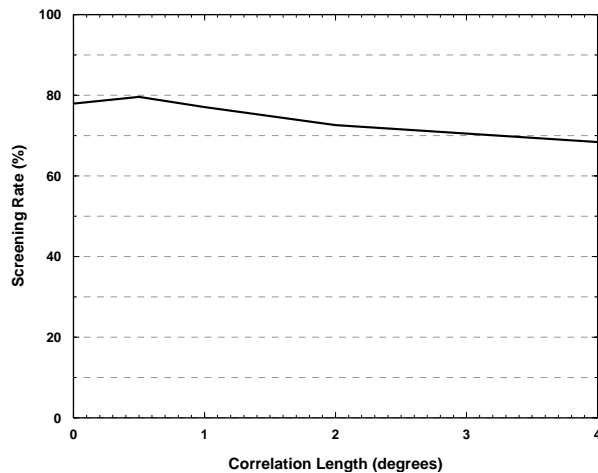


**Figure 9. Percentage of earthquakes worldwide that are rejected as being *explosion-like* at the 0.005 significance level as a function of  $\alpha_r$ .**

## **CONCLUSIONS AND RECOMMENDATIONS**

We acquired and processed spectra for earthquake pairs and/or clusters prior to 2000, based on waveform cross-correlation results from Schaff. Preliminary results indicate that estimated corner frequencies for regional P and S waves from earthquakes are very similar for a majority of the events. In conjunction with results by Fisk (2006, 2007), this may explain the frequency dependence of P/S discriminants. It may also allow more robust fitting of Brune source model parameters, using a broader range of frequencies, by combining relative spectra of regional P and S phases for earthquakes.

We are extending this analysis to event pairs in Eurasia since 2000. Using the Preliminary Determination of Epicenters (PDE) catalog, we formed a list of candidate pairs, based on proximity, and acquired regional data from IRIS for the events. We then computed waveform cross-correlations to find pairs with similar waveforms. We processed and fit network-averaged relative spectra for almost 3600 pairs of events. We have automated all of these processing steps. We are performing quality control of the results, which we plan to merge with our previous results to obtain more extensive estimates of corner frequencies and stress-drop parameters for Eurasia. We also plan to examine uncertainties in these estimates and begin estimating Q and geometrical spreading parameters with source terms fixed.

We also studied the impact of using event clusters with anomalous P/S data for kriging. In the worst scenario, using only RV events to calibrate NTS for KNB, 11 of 88 UNEs were mis-categorized as *earthquake-like* because the RV events have very high Pn/Lg values ( $2.4\sigma$  above the global earthquake average) at KNB and the posterior calibration variance computed by the old method is small, treating the RV events as independent. Since the RV earthquakes had similar mechanisms, mainly left lateral strike-slip faulting on northeast-striking high-angle structures (Smith and Brune, 1993), it is invalid to treat them as independent. Although the procedure of Bottone et al. (2002) was used for this study, the problem is inherent to any kriging method that does not treat intrinsic correlations of clustered calibration data.

We showed that the new kriging method, that introduces a second correlation length, limits the effective number of reference samples for clustered events. This extension keeps the corrections from weighting local clusters too highly and the posterior calibration variance from being too small. We showed that the new method did not mis-categorize any NTS UNEs, even when replicating the set of RV events 20 times. Thus, the extended method seems very robust. Although many events were *undetermined* for this case, this is the appropriate result, based on the reference data. Fortunately, such cases are rare ( $<1\%$  for  $2.4\sigma$ ). In fact, application to global data sets shows that the power of the test to reject earthquakes as explosions did not degrade much, even for conservatively large values of  $\alpha_r$ . Thus, a practical solution to this problem is available (e.g., using a conservative value of  $\alpha_r = 1.0$ ) and it provides useful monitoring performance. Further work is needed to estimate  $\alpha_r$ . Although this does not seem necessary for the global case, application to specific sites may improve significantly by using site-specific values. We plan to analyze relevant data for earthquake clusters in Eurasia to examine this issue.

## **ACKNOWLEDGMENTS**

We thank Gary McCartor and Steve Bottone for many useful discussions, Bill Walter of LLNL for regional seismic amplitudes for NTS events, Ward Hawkins of LANL for seismic data for events in Eurasia, and David Schaff for waveform cross-correlation values. We also acknowledge the IRIS DMC for data used in this study.

**REFERENCES**

- Bottone, S., M. D. Fisk and G. D. McCartor (2002). Regional seismic event characterization using a Bayesian formulation of simple kriging, *Bull. Seism. Soc. Am.* 92: 2277–2296.
- Brune, J. N. (1970). Tectonic stress and the spectra of seismic shear waves from earthquakes, *J. Geophys. Res.* 75: 4997–5009.
- Choy and Boatwright (1995). Global patterns of radiated seismic energy and apparent stress, *J. Geophys. Res.* 100: 18,205–18,228.
- Cong, L., J. Xie and B. J. Mitchell (1996). Excitation and propagation of Lg from earthquakes in central Asia with implications for explosion/earthquake discrimination, *J. Geophys. Res.* 101: 27,779–27,789.
- Fan G-W., T. Lay and S. Bottone (2002). Path corrections for source discriminants: a case study at two international seismic monitoring stations, *Pure and Appl. Geophys., Special Edition on Monitoring the Comprehensive Nuclear-Test-Ban Treaty: Seismic Event Discrimination and Identification* 159: 651–678.
- Fisk, M. D. (2007). Corner Frequency Scaling of Regional Seismic Phases for Underground Nuclear Explosions at the Nevada Test Site, *Bull. Seism. Soc. Am.*: 97: 977–988.
- Fisk, M. D. (2006). Source spectral modeling of regional P/S discriminants at nuclear test sites in China and the Former Soviet Union, *Bull. Seism. Soc. Am.* 96: 2348–2367.
- Fisk, M. D., S. Bottone, and G. D. McCartor (2001). Regional Seismic Event Characterization Using Bayesian Calibration, MRC-R-1621, Mission Research Corp., Santa Barbara, CA.
- Madariaga, R. (1976). Dynamics of an expanding circular fault, *Bull. Seism. Soc. Am.* 66: 639–667.
- Nuttli, O. W. (1983). Average seismic source-parameter relations for mid-plate earthquakes, *Bull. Seism. Soc. Am.* 73: 519–535.
- Phillips, W. S. (1999). Empirical path corrections for regional seismic phases, *Bull. Seism. Soc. Am.* 89: 384–393.
- Phillips, W. S., G. E. Randall and S. R. Taylor (1998). Path correction using interpolated amplitude residuals: An example from central China, *Geophys. Res. Lett.* 25: 2729–2732.
- Rodgers, A. J., T. Lay, G. Fan and W. R. Walter (1998). Calibration of distance and path effects on regional P/S discriminants at station ABKT (Alibek, Turkmenistan): statistical analysis of crustal waveguide effects, UCRL-JC-129165, Lawrence Livermore National Laboratory.
- Rodgers, A. J., W. R. Walter, C. A. Schultz, S. C. Myers, and T. Lay (1999). A comparison of methodologies for representing path effects on regional P/S discriminants, *Bull. Seism. Soc. Am.* 89: 394–408.
- Schaff, D. P. and P. G. Richards (2004). Repeating seismic events in China, *Science* 303: 1176–1178.
- Smith, K. D. and J. N. Brune (1993). A sequence of very shallow earthquakes in the Rock Valley fault zone; southern Nevada test site, *EOS Suppl.* 74: 417.
- Taylor, S. R., and H. E. Hartse (1998). A procedure for estimation of source and propagation amplitude corrections for regional seismic discriminants, *J. Geophys. Res.* 103: 2781–2789.
- Taylor, S. R., A. A. Velasco, H. E. Hartse, W. S. Phillips, W. R. Walter, and A. J. Rodgers (2002). Amplitude corrections for regional seismic discriminants, *Pure and Appl. Geophys., Special Edition on Monitoring the Comprehensive Nuclear-Test-Ban Treaty: Seismic Event Discrimination and Identification* 159: 623–650.
- Walter, W. R., K. M. Mayeda, and H. J. Patton (1995). Phase and spectral ratio discrimination between NTS earthquakes and explosions. Part I: Empirical observations, *Bull. Seism. Soc. Am.*, 85, 1050–1067.
- Walter, W. R. and S. R. Taylor (2002). A Revised Magnitude and Distance Amplitude Correction (MDAC2) Procedure for Regional Seismic Discriminants: Theory and Testing at NTS, *UCRL-ID-146882*, LA-UR-02-1008.